Supporting information for

Assessing the Impact of Electronic and Steric Tuning of the Ligand in the Spin State and Catalytic Oxidation Ability of the Fe^{II}(Pytacn) Family of Complexes

Irene Prat[a], Anna Company[a,*], Teresa Corona[a], Teodor Parella[b], Xavi Ribas[a], Miquel Costas[a,*]

[a]Grup de Química Bioinorgànica i Supramolecular (QBIS). Institut de Química Computacional i Catàlisi (IQCC). Departament de Química. Universitat de Girona. Campus Montilivi, E17071 Girona, Catalonia (Spain). anna.company@udg.edu, miquel.costas@udg.edu

[b]Servei de Ressonància Magnètica Nuclear, Universitat Autònoma de Barcelona, Bellaterra, E08193 Barcelona (Spain)

Contents

1. Synthesis of ligands 2
2. Solid state characterization 4
   2.1. X-ray structures 4
   2.2. SQUID measurement 7
3. Paramagnetic ^{1}H-NMR 8
4. References 15

1. Synthesis of ligands

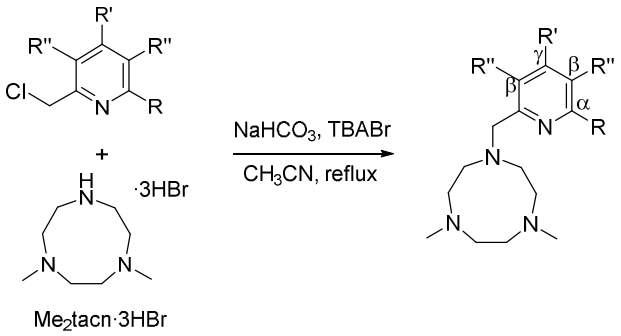

ligand	R	R'	R''
^{H,H}Pytacn	H	H	H
^{H,NMe2}Pytacn	H	NMe_2	H
^{H,OMe}Pytacn	H	OMe	Me
^{H,Me}Pytacn	H	Me	H
^{H,Cl}Pytacn	H	Cl	H
^{H,CO2Et}Pytacn	H	CO_2Et	H
^{H,NO2}Pytacn	H	NO_2	H
^{Me,H}Pytacn	Me	H	H
^{Me,Me}Pytacn	Me	Me	H
^{Cl,H}Pytacn	Cl	H	H
^{F,H}Pytacn	F	H	H

Scheme S1. Synthesis and nomenclature of the ligands used in this work.

Me_2tacn·3HBr,[1] ^{H,H}Pytacn,[2] ^{Me,H}Pytacn,[3] ^{H,Me}Pytacn,[4] ^{H,NMe2}Pytacn,[4] ^{H,Cl}Pytacn,[4] ^{H,NO2}Pytacn,[4] ^{Me,Me}Pytacn[4], ^{Cl,H}Pytacn,[4] and ^{F,H}Pytacn[4] were synthesized as previously described.

Synthesis of 1-[(3,5-dimethyl-4-methoxy-2-pyridyl)methyl]-4,7-dimethyl-1,4,7-triazacyclononane (^{H,OMe}Pytacn)

Commercially available (chloromethyl)-4-methoxy-3,5-dimethylpyridine (0.28 g, 1.3 mmol), Me_2tacn·3HBr (0.50 g, 1.3 mmol) and anhydrous acetonitrile (25 mL) were mixed in a 50 mL flask. Na_2CO_3 (0.96 g) and tetrabutylammonium bromide, TBABr (0.03 g) were added directly as solids and the resulting mixture was heated at reflux under N_2 for 16 hours. After cooling to room temperature, the resulting yellow mixture was filtered and the filter cake was washed with CH_2Cl_2. The combined filtrates were evaporated under reduced pressure. To the resulting residue, 1M NaOH (30 mL) was added and the mixture was extracted with CH_2Cl_2 (3 x 10 mL). The combined organic layers were dried over anhydrous $MgSO_4$ and the solvent was removed under reduced pressure. The resulting residue was treated with hexane (70 mL) and stirred for 12 hours. The mixture was filtered and the solvent from the yellow filtrates was removed under reduced pressure to yield the product as a pale yellow oil (0.25 g, 1.6 mmol, 66 %). FT-IR (ATR) ν, cm^{-1}: 2925 – 2808 $(C\text{-}H)_{sp3}$, 1671, 1454 (py). ^{1}H-NMR ($CDCl_3$, 400 MHz, 300K) δ, ppm: 8.15 (s, 1H, py**H**$_\alpha$), 3.77 (s, 3H, O-C**H$_3$**), 3.71 (s, 2H, py-C**H$_2$**), 2.82 – 2.78 (m, 4H, N-C**H$_2$**-CH_2), 2.64 (s, 4H, N-C**H**$_2$-CH_2), 2.62 - 2.59 (m, 4H, N-C**H**$_2$-CH_2), 2.38 (s, 3H, py-**CH$_3$**), 2.31 (s, 6H, N-C**H$_3$**), 2.24

(s, 3H, py-C**H$_3$**). ^{13}C-NMR ($CDCl_3$, 75 MHz, 300K) δ, ppm: 164.10 (py**C**$_q$), 157.75 (py**C**$_\gamma$), 148.25 (py**C**$_\alpha$), 126.10, 124.90 (py**C**$_\beta$), 63.73 (py-OC**H$_3$**), 59.74 (py-**C**H$_2$-N), 57.01, 56.46, 56.10 (N-**C**H$_2$-C), 46.34 (N-**C**H$_3$), 13.20, 11,27 (py-**C**H$_3$). ESI-MS (m/z): 307.2 $[M+H]^+$.

Synthesis of 1-[(4-ethoxycarbonyl-2-pyridyl)methyl]-4,7-dimethyl-1,4,7-triazacyclononane (^{H,CO2Et}Pytacn)

2-chloromethyl-4-ethoxycarbonylpyridine hydrochloride. To a stirred solution of commercially available 4-ethoxycarbonyl-2-hydroxymethylpyridine (0.64 g, 3.5 mmol) in CH_2Cl_2 (25 mL) was added thionyl chloride (1.3 mL, 17.8 mmol) dropwise. After the addition, the resulting mixture was stirred at room temperature for 16 h. The solvent was removed by bubbling N_2 into the crude mixture (gaseous HCl is formed during this process and extreme cautions must be taken) and a white solid was obtained. This product was suspended in diethyl ether (20 mL) which caused the formation of a solid. This compound was filtered and dried under vacuum. The desired product was obtained as a white solid (0.59 g, 2.5 mmol, 71%). ^{1}H NMR (400 MHz, $CDCl_3$): δ 8.78 (d, J = 5.5 Hz, 1H), 8.40 (s, 1H), 8.20 (d, J = 5.5 Hz, 1H), 5.10 (s, 2H), 4.52 (q, J = 7.1 Hz, 2H), 1.46 (t, J = 7.1 Hz, 3H).

1-[(4-ethoxycarbonyl-2-pyridyl)methyl]-4,7-dimethyl-1,4,7-triazacyclononane (^{H,CO2Et}Pytacn). This ligand was prepared in analogous manner to ^{H,OMe}Pytacn but using 2-chloromethyl-4-ethoxycarbonylpyridine hydrochloride. Yield = 77%. FT-IR (ATR) ν, cm^{-1}: 2924 – 2785 $(C\text{-}H)_{sp3}$, 1727 (C=O), 1452 (py). ^{1}H-NMR ($CDCl_3$, 400 MHz, 300K) δ, ppm: 8.67 (dd, J = 5.1 Hz, J' = 0.9 Hz, 1H, py**H**$_\alpha$), 8.07 (s, 1H, py**H**$_{\beta'}$), 7.70 (dd, J = 5.2 Hz, J' = 1.6 Hz, 1H, py**H**$_\beta$), 4.42 (q, J = 7.0 Hz, 2H, OC**H$_2$**CH$_3$), 3.91 (s, 2H, py-C**H$_2$**), 2.85 - 2.83 (m, 4H, N-C**H$_2$**-CH$_2$), 2.78 (s, 4H, N-C**H$_2$**-CH$_2$), 2.69 - 2.67 (m, 4H, N-C**H$_2$**-CH$_2$), 2.36 (s, 6H, N-C**H$_3$**), 1.40 (t, J = 7.0 Hz, 3H, OCH$_2$C**H$_3$**). ^{13}C-NMR ($CDCl_3$, 75 MHz, 300K) δ, ppm: 165.45 (**C**=O), 161.82 (py**C**$_q$), 149.70 (py**C**$_\gamma$), 138.00 (py**C**$_\alpha$), 122.49, 120.98 (py**C**$_\beta$), 64.47 (py-**C**H$_2$-N), 61.69 (CO_2**C**H$_2$CH$_3$), 57.14, 57.03, 56.12 (N-**C**H$_2$-C), 46.66 (N-**C**H$_3$), 14.22 (CO_2CH_2**C**H$_3$). ESI-MS (m/z): 321.2 $[M+H]^+$.

2. Solid state characterization

2.1. X-ray structures

Figure S1. X-Ray structures of ^{Cl,H}**1**, ^{H,Me}**1** and ^{H,Cl}**1**.

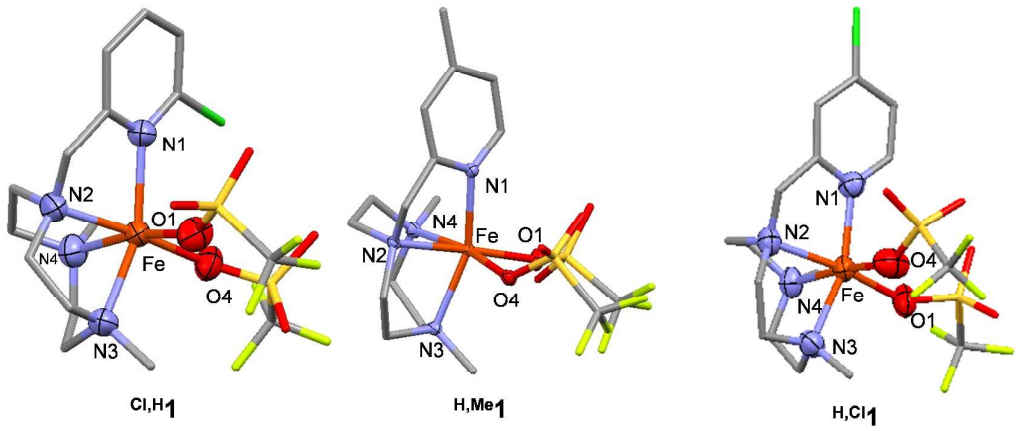

Table S1. Crystal data for ^{Cl,H}**1**, ^{H,Me}**1** and ^{H,Cl}**1**.

	^{Cl,H}**1**	^{H,Me}**1**	^{H,Cl}**1**
Empirical formula	$C_{17}H_{25}Cl_3F_6FeN_4O_6S_2$	$C_{17}H_{26}F_6FeN_4O_6S_2$	$C_{16}H_{23}ClF_6FeN_4O_6S_2$
Formula weight	721.73	616.39	636.80
Temperature	298(2) K	100(2) K	300(2) K
Wavelength	0.71073 A	0.71073 Å	0.71073 Å
Crystal system	Orthorhombic	Orthorombic	Monoclinic
Space group	$P2_12_12_1$	$P2_12_12_1$	$P2_1/c$
Unit cell dimensions	a = 8.738(2) Å	a = 8.550(3) Å	a = 8.965(2)
	α = 90º	α = 90º	α = 90º
	b = 16.228(4) Å	b = 13.577(5) Å	b = 25.125(5) Å
	β = 90º	β = 90.00º	β = 123.939(11)º
	c = 20.412(6) Å	c = 21.298(8) Å	c = 13.422(3) Å
	γ = 90º	γ = 90.00º	γ = 90.00º
Volume	2894.3(13) A^3	2472.3(16) $Å^3$	2517.8(16) $Å^3$
Density (calculated)	1.656 $g\cdot cm^{-3}$	1.656 $g\cdot cm^{-3}$	1.680 $g\cdot cm^{-3}$
Absorption coefficient	1.020 mm^{-1}	0.865 mm^{-1}	0.955 mm^{-1}
F(000)	1464	1264	1296
Cell formula units_Z	4	4	4
Crystal size	0.3 x 0.25 x 0.2 mm	0.5 x 0.2 x 0.2 mm	0.3 x 0.2 x 0.2 mm
Θ range for data collection	2.00 to 28.29º	1.78 to 28.40º	1.99 to 28.36º
Limiting indices	-11<=h<=11,	-11<=h<=11	-11<=h<=11
	-21<=k<=21,	-18<=k<=18	-33<=k<=33
	-27<=l<=27	-28<=l<=28	-17<=l<=17
Reflections collected	45303	38665	39322
Independent reflections	7156 [R(int) = 0.0558]	6147 [R(int) = 0.0529]	6201 [R(int) = 0.0245]
Completeness to Θ	99.6 %	99.5 % (Θ = 28.40º)	98.9 % (Θ = 28.36º)
Refinement method	Full-matrix least-squares on F^2	Full-matrix least-squares on F^2	Full-matrix least-squares on F^2
Data/restraints/parameters	7156 / 0 / 325	6147 / 0 / 328	6201 / 0 / 325
Goodness-of-fit on F^2	0.993	1.077	1.057
Final R indices [I>2σ(I)]	R1 = 0.0460,	R1 = 0.0257	R1 = 0.0447
	wR2 = 0.1127	wR2 = 0.0582	wR2 = 0.1310
R indices (all data)	R1 = 0.0605,	R1 = 0.0299	R1 = 0.0512
	wR2 = 0.1197	wR2 = 0.0593	wR2 = 0.1355
Largest diff. peak and hole	0.320 and -0.245 $e.A^{-3}$	0.346 and -0.261 $e.Å^{-3}$	0.617 and -0.447 $e.Å^{-3}$

Table S2. Selected bond lengths (Å) and angles (º) for ^{Cl,H}**1**, ^{H,Me}**1** and ^{H,Cl}**1**.

^{Cl,H}1		^{H,Me}1		^{H,Cl}1	
Fe-N1	2.258(2)	Fe-N1	2.1608(16)	Fe-N1	2.163(2)
Fe-N2	2.193(3)	Fe-N2	2.1924(15)	Fe-N2	2.2141(19)
Fe-N3	2.217(3)	Fe-N3	2.2062(15)	Fe-N3	2.193(2)
Fe-N4	2.226(3)	Fe-N4	2.2505(16)	Fe-N4	2.223(2)
Fe-O1	2.157(2)	Fe-O1	2.0610(14)	Fe-O1	2.0654(18)
Fe-O4	2.053(2)	Fe-O4	2.1604(14)	Fe-O4	2.161(2)
N2-Fe-N1	74.93(10)	N1-Fe-N2	77.61(6)	N1-Fe-N2	77.76(8)
N3-Fe-N1	153.53(11)	N1-Fe-N4	94.45(6)	N1-Fe-N4	100.52(8)
O4-Fe-N1	108.48(10)	N1-Fe-O4	90.31(5)	N1-Fe-O4	85.68(8)
O1-Fe-N1	86.52(10)	N1-Fe-O1	104.89(6)	N1-Fe-O1	107.86(8)
N2-Fe-N4	79.70(12)	N4-Fe-N2	80.08(6)	N4-Fe-N2	80.00(8)
N3-Fe-N4	80.09(11)	N4-Fe-N3	80.47(6)	N4-Fe-N3	81.27(8)
O4-Fe-N4	92.07(11)	N2-Fe-O4	91.56(5)	N2-Fe-O4	98.32(10)
O1-Fe-N4	168.71(11)	N4-Fe-O1	99.51(6)	N4-Fe-O1	89.47(8)
O1-Fe-N2	98.93(11)	N3-Fe-O1	97.41(6)	N3-Fe-O1	94.54(9)
N2-Fe-N3	80.17(10)	N2-Fe-N3	80.09(6)	N2-Fe-N3	80.53(8)
O4-Fe-N4	92.07(11)	N3-Fe-O4	91.49(5)	N3-Fe-O4	91.76(8)
O4-Fe-O1	88.93(10)	O4-Fe-O1	88.54(5)	O4-Fe-O1	91.72(10)

Figure S2. X-Ray structures of ^{H,CO2Et}**1** and ^{H,OMe}**1**.

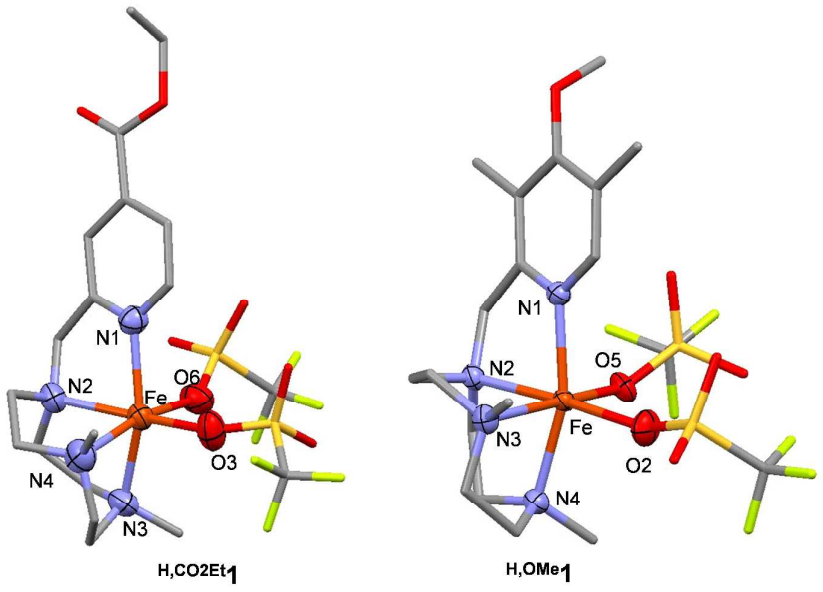

Table S3. Crystal data for ^{H,CO2Et}**1** and ^{H,OMe}**1**.

	^{H,CO2Et}**1**	^{H,OMe}**1**
Empirical formula	$C_{19}H_{28}F_6FeN_4O_8S_2$	$C_{19}H_{30}F_6FeN_4O_7S_2$
Formula weight	674.42	660.44
Temperature	300(2) K	150(2) K
Wavelength	0.71073 Å	0.71073 Å
Crystal system	Monoclinic	Monoclinic
Space group	$P2_1/c$	$P2_1/c$
Unit cell dimensions	a = 12.949(3) Å	a = 18.558 (11) Å
	α = 90º	α = 90º
	b = 24.597(6) Å	b = 9.011(5) Å
	β = 96.489(6)°	β = 118.798(9)º
	c = 8.910(2) Å	c = 19.218(11) Å
	γ = 90º	γ = 90.00º
Volume	2819.5(12) $Å^3$	2816(3) $Å^3$
Density (calculated)	1.589 $g{\cdot}cm^{-3}$	1.558 $g{\cdot}cm^{-3}$
Absorption coefficient	0.771 mm^{-1}	0.768 mm^{-1}
F(000)	1384	1360
Cell formula units_Z	4	4
Crystal size	0.4 x 0.15 x 0.08 mm	0.4 x 0.25 x 0.1 mm
Θ range for data collection	2.70 to 28.28°	2.12 to 28.23º
Limiting indices	-17<=h<=17	-24<=h<=24
	-32<=k<=32	-11<=k<=11
	-11<=l<=11	-25<=l<=25
Reflections collected	21941	42154
Independent reflections	6844 [R(int) = 0.0347]	6886 [R(int) = 0.0399]
Completeness to Θ	99.1% (Θ = 28.28º)	99.1% (Θ = 28.23º)
Refinement method	Full-matrix least-squares on F^2	Full-matrix least-squares on F^2
Data/restraints/parameters	6844 / 2 / 361	6886 / 0 / 357
Goodness-of-fit on F^2	0.995	1.028
Final R indices [I>2σ(I)]	R1 = 0.0434	R1 = 0.0409
	wR2 = 0.0998	wR2 = 0.1066
R indices (all data)	R1 = 0.0580	R1 = 0.0506
	wR2 = 0.1093	wR2 = 0.1142
Largest diff. peak and hole	0.386 and -0.239 e. $Å^{-3}$	0.714 and -0.459 e. $Å^{-3}$

Table S4. Selected bond lengths (Å) and angles (º) for ^{H,CO2Et}**1** and ^{H,OMe}**1**.

^{H,CO2Et}**1**		^{H,OMe}**1**	
Fe-N1	2.177(3)	Fe-N1	2.1387(19)
Fe-N2	2.199(3)	Fe-N2	2.2007(19)
Fe-N3	2.188(3)	Fe-N3	2.252(2)
Fe-N4	2.226(3)	Fe-N4	2.182(2)
Fe-O3	2.208(3)	Fe-O2	2.0597(19)
Fe-O6	2.035(2)	Fe-O5	2.1813(17)
N1-Fe-N2	76.24(10)	N1-Fe-N2	77.56(7)
N1-Fe-N3	153.38(11)	N1-Fe-N4	159.25(7)
N1-Fe-O6	100.23(11)	N1-Fe-O5	87.45(7)
N1-Fe-O3	83.82(10)	N1-Fe-O2	105.82(7)
N4-Fe-N2	79.95(12)	N4-Fe-N2	81.69(7)
N4-Fe-N3	80.61(13)	N4-Fe-N3	81.05(8)
N4-Fe-O6	90.42(12)	N2-Fe-O5	89.31(7)
N4-Fe-O3	166.52(12)	N4-Fe-O2	94.92(7)
N2-Fe-O3	98.92(11)	N3-Fe-O2	97.84(8)
N2-Fe-N3	81.20(11)	N2-Fe-N3	80.36(7)
N3-Fe-O6	104.65(13)	N3-Fe-O5	168.43(6)
O4-Fe-O1	92.16(11)	O5-Fe-O2	92.17(8)

2.2. SQUID measurement

Figure S3. Temperature dependence of $\chi_m T$ for solid ^{Me,H}**2**SbF_6.

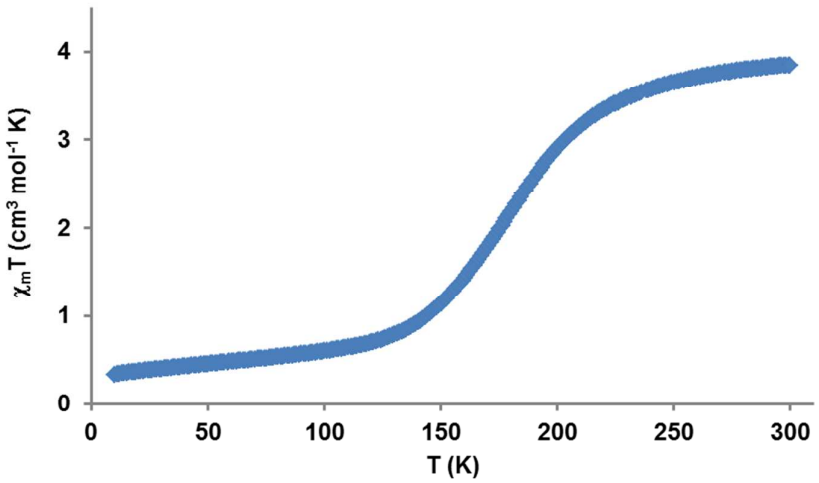

Magnetization measurements of a solid sample of ^{Me,H}**2**SbF_6 in an applied field of 100 Oe in the temperature range 10-300 K confirm the spin crossover of the iron(II) center observed by X-Ray analysis from high-spin to low-spin. The $\chi_m T$ product decreases upon cooling, from 3.8 $cm^3mol^{-1}K$ at 300 K down to 0.3 $cm^3mol^{-1}K$ at 10 K. The spin crossover is centered at 170 K and it occurs over a temperature range of 100 K. These magnetization measurements indicate that the spin crossover is virtually complete at 100 K, as previously established by X-Ray analysis (Figure 2).

3. Paramagnetic ^{1}H-NMR

Figure S4. ^{1}H-NMR spectra of triflate complexes $^{H,R'}$**1** in CD_2Cl_2.

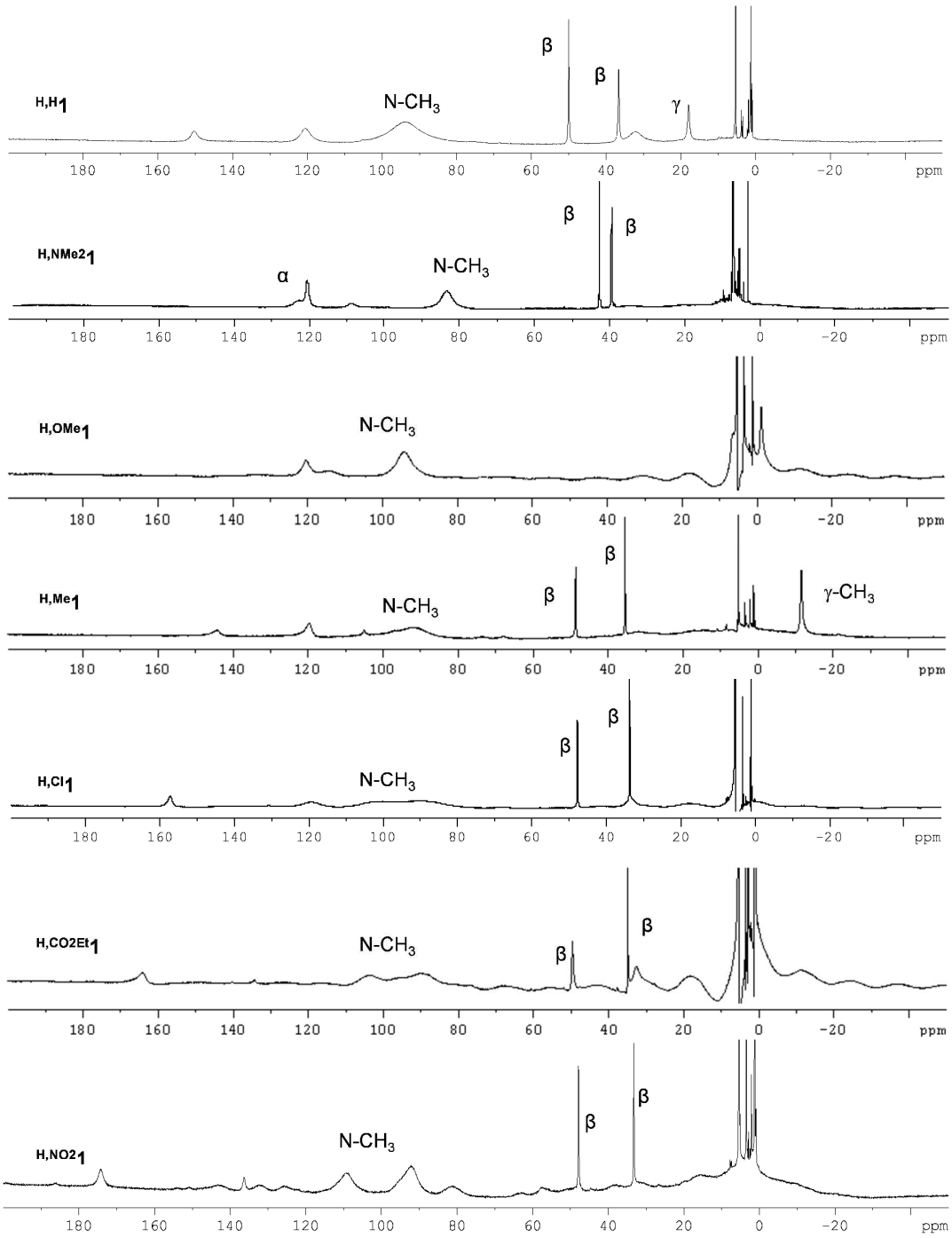

Figure S5. ^{1}H-NMR spectra of triflate complexes ^{R,H}**1** (R = Me, Cl, F) in CD_2Cl_2.

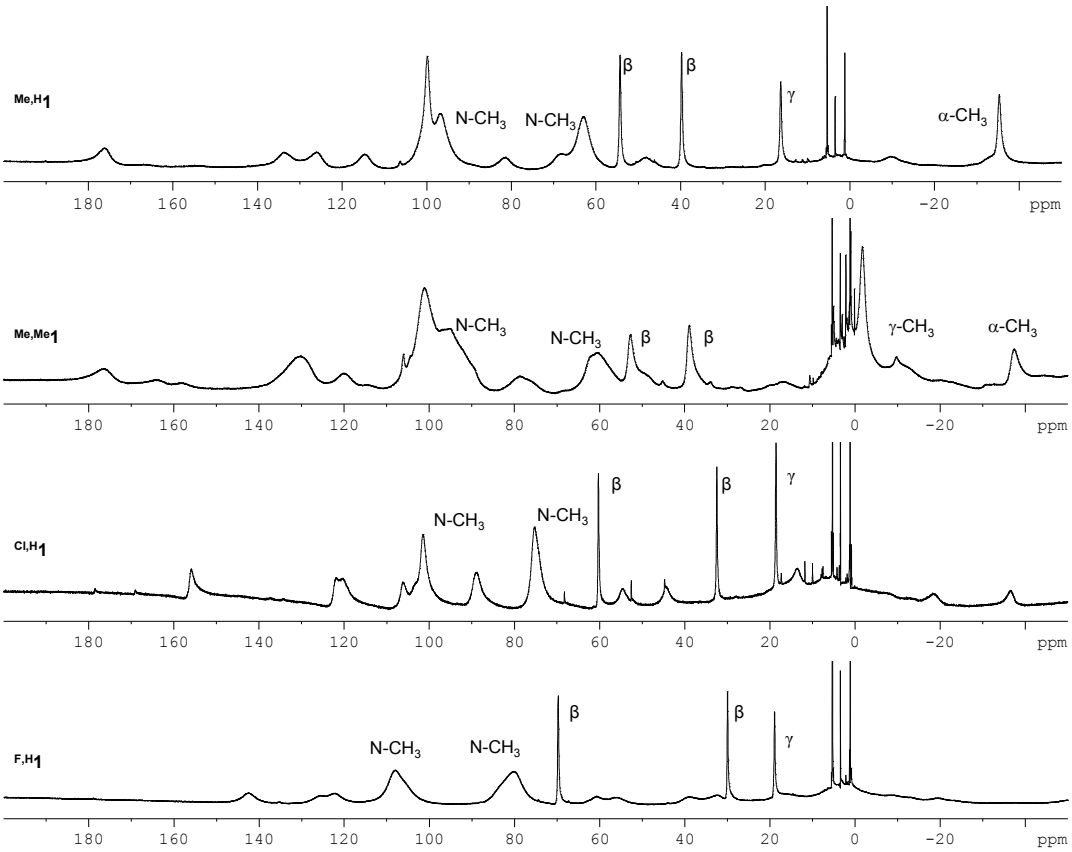

Figure S6. ^{1}H-NMR spectrum of ^{Me,H}**1** in CD_2Cl_2 at different temperatures.

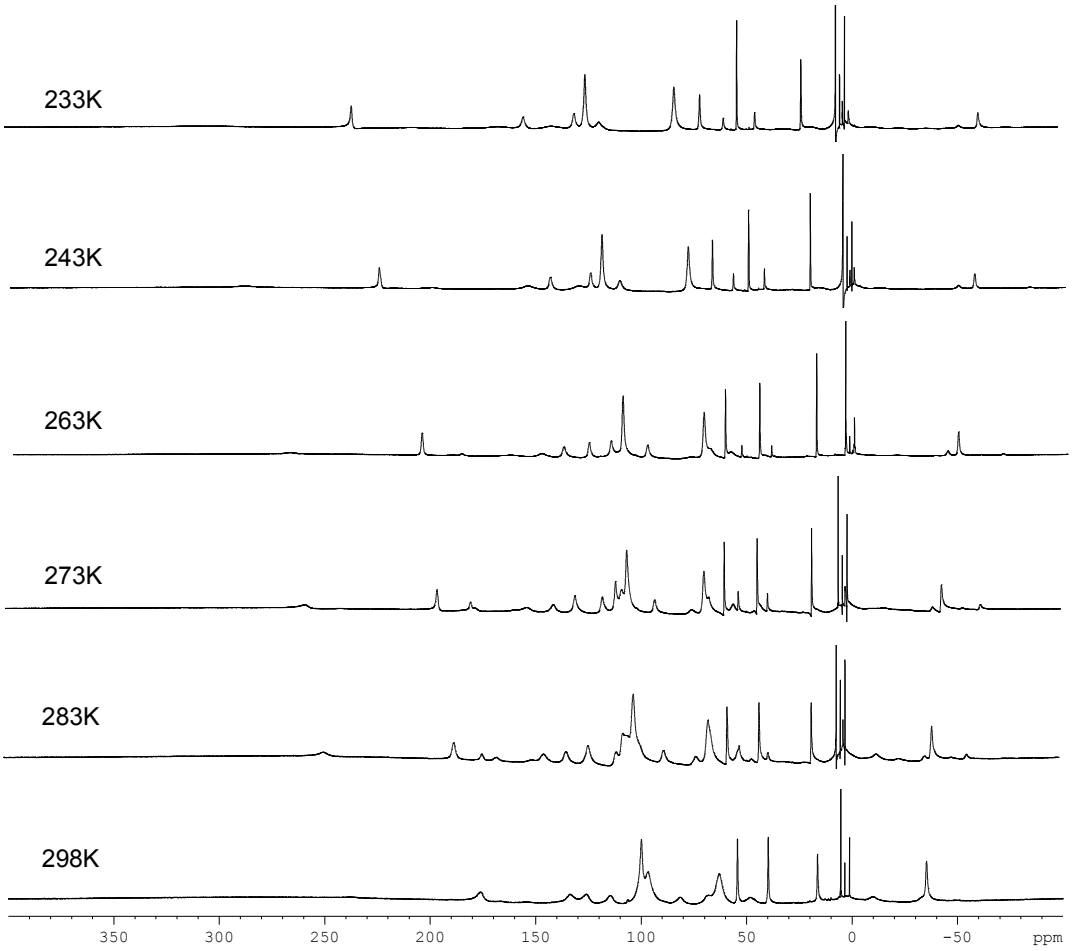

Figure S7. Representation of the chemical shift in front of temperature of selected signals in the ^{1}H-NMR spectrum of complex ^{Me,H}**1** in CD_2Cl_2. The paramagnetic shift of the protons is linearly dependent on the inverse of the temperature, which is indicative of a Curie behavior.

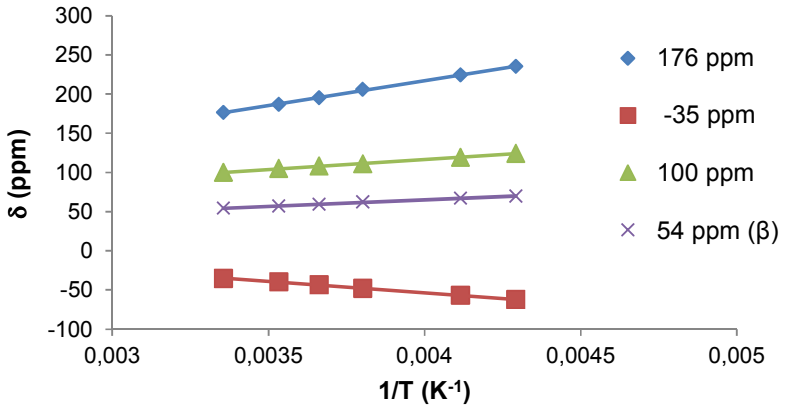

Figure S8. ^{1}H-NMR spectrum of ^{H,H}**2**SbF_6 in CD_3CN at -30ºC and 25ºC along with the aromatic region of the COSY spectrum measured at 25ºC.

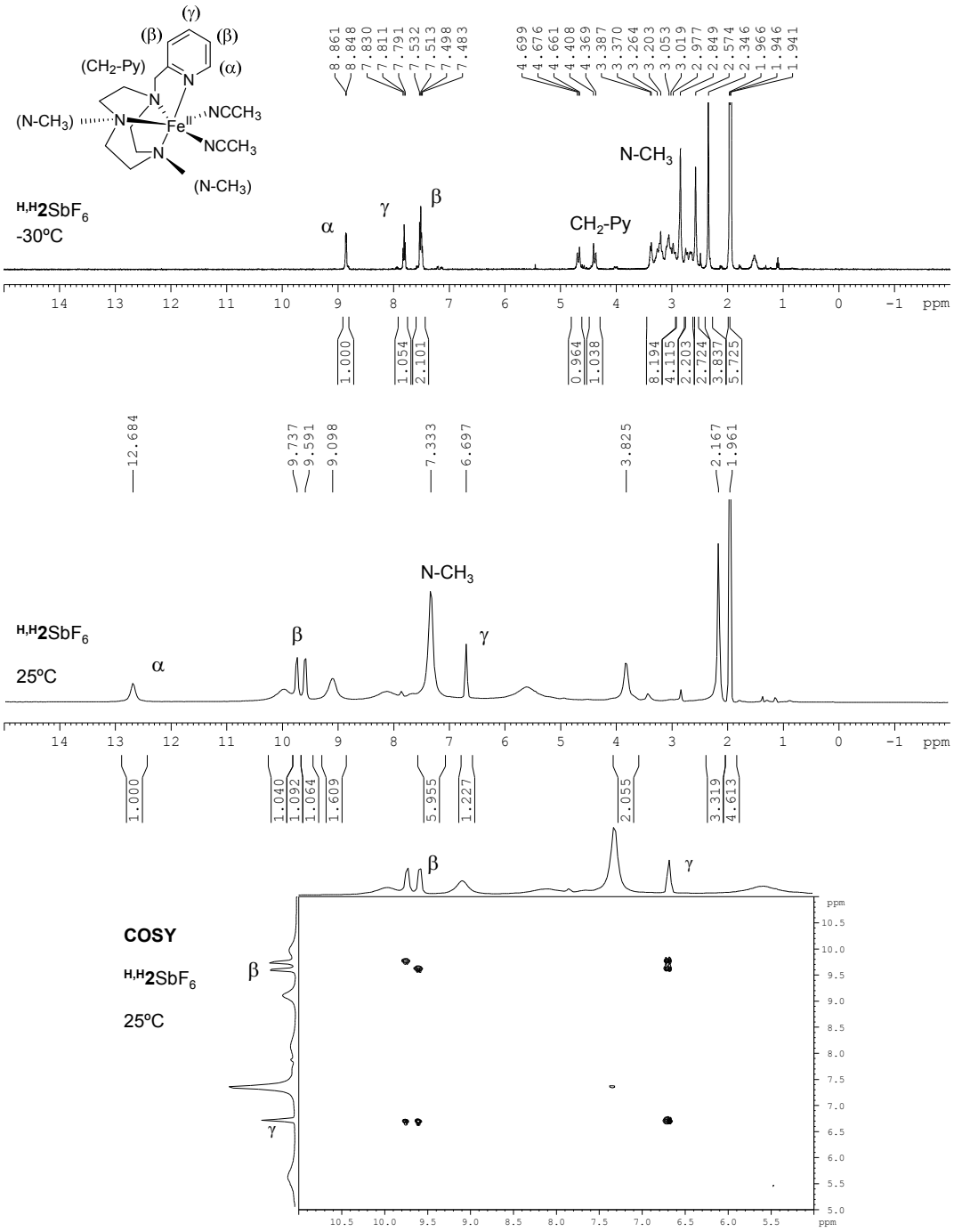

Figure S9. ^{1}H-NMR spectrum of ^{Me,H}**2**SbF_6 in CD_3CN at room temperature.

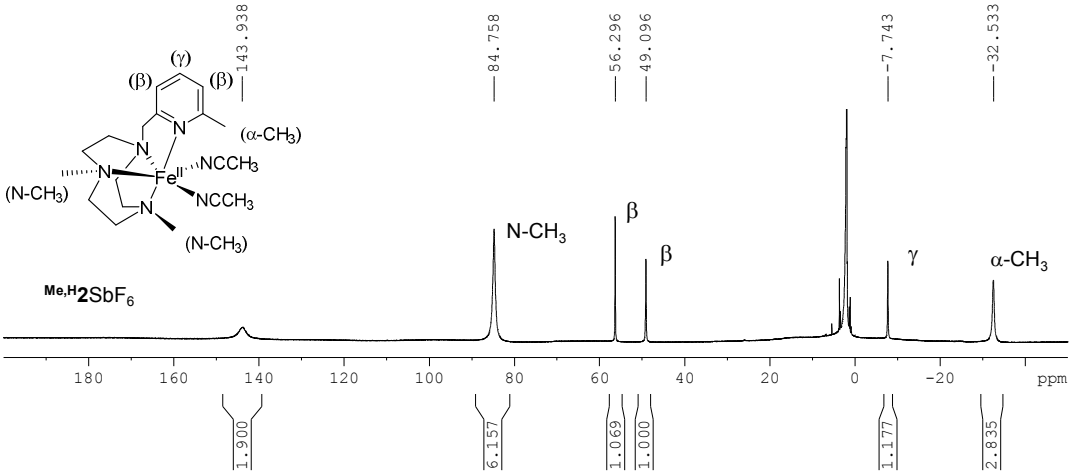

Figure S10. ^{1}H-NMR spectra of triflate complexes $^{H,R'}$**1** in CD_3CN. The triflate anions are replaced by acetonitrile molecules, thus, in solution the bis-acetonitrile complexes $^{H,R'}$**2**OTf are formed.

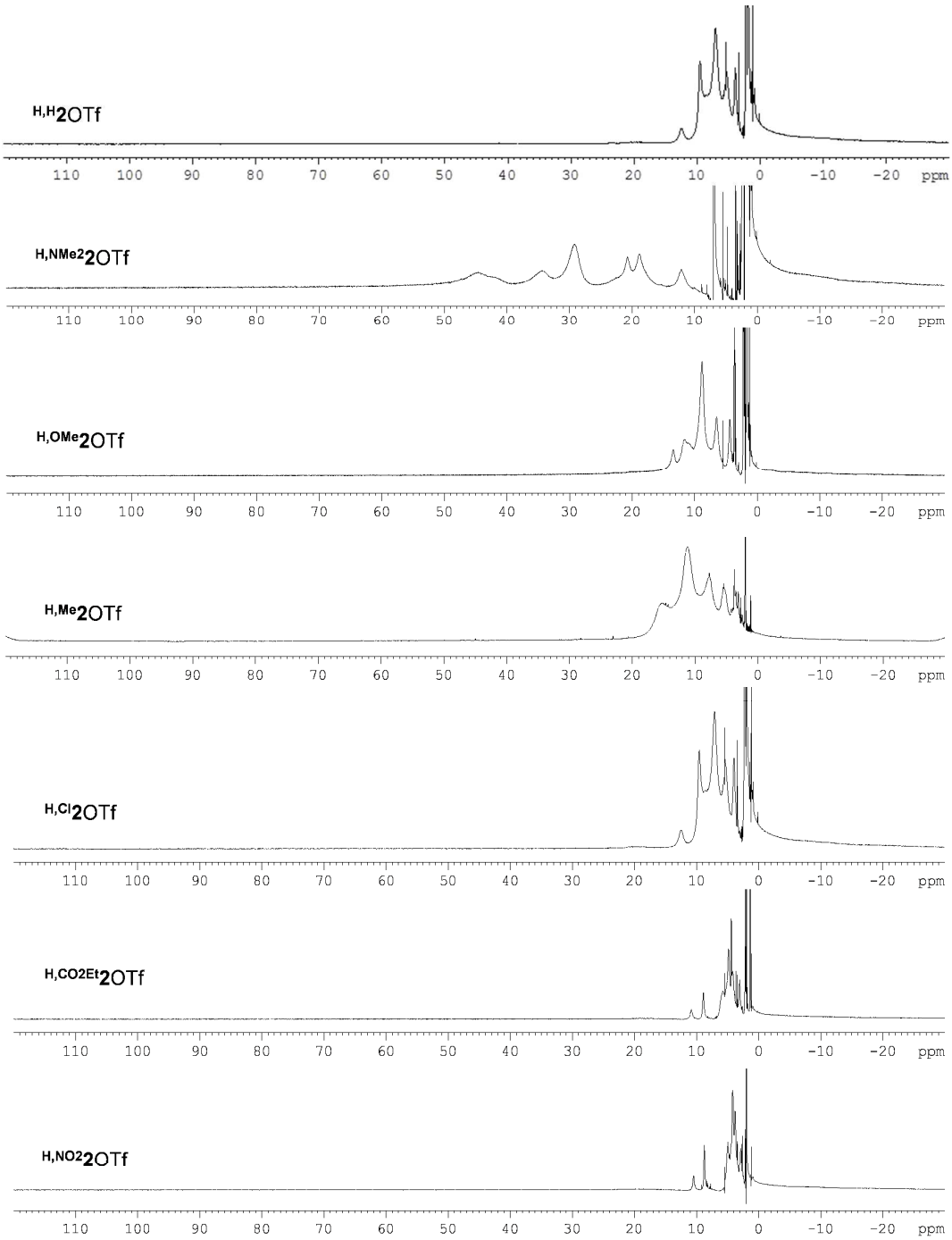

Figure S11. ^{1}H-NMR spectra of triflate complexes ^{R,H}**1** (R = Me, Cl, F) in CD_3CN. The triflate anions are replaced by acetonitrile molecules, thus, in solution the bis-acetonitrile complexes ^{R,H}**2**OTf are formed.

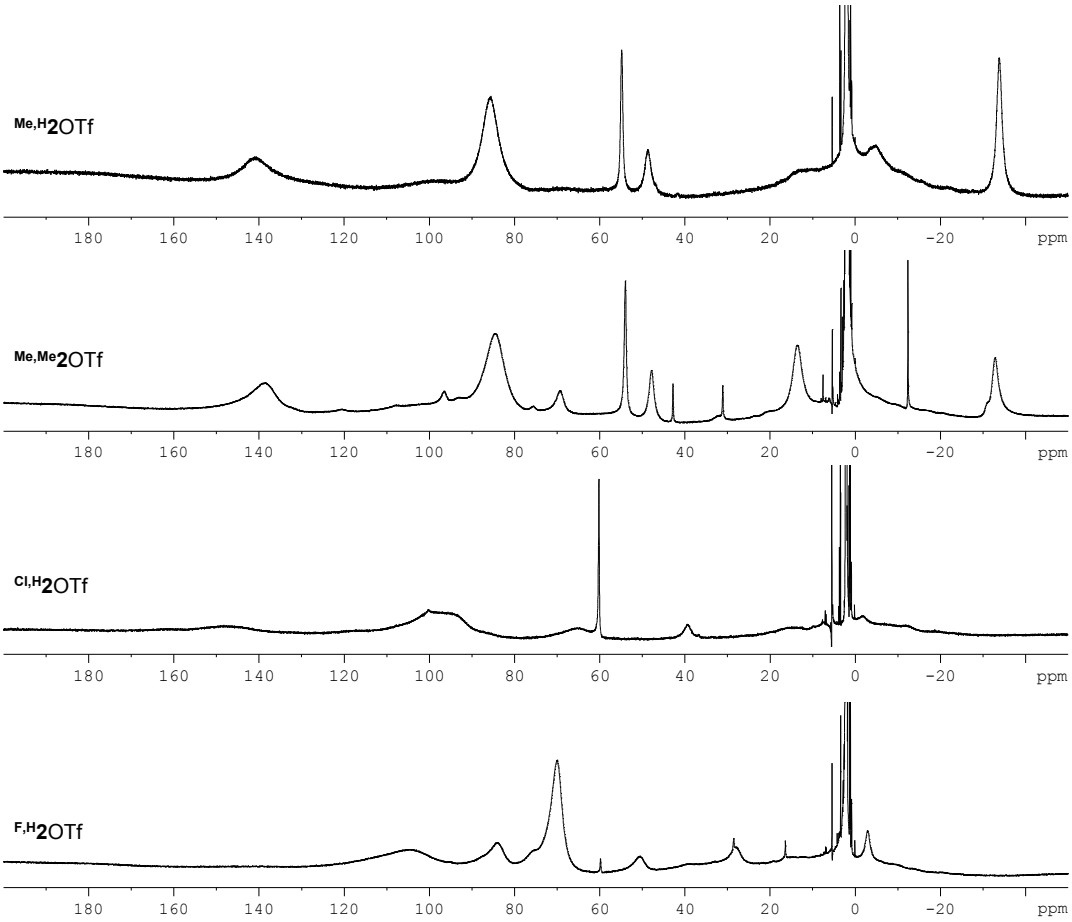

4. References

[1] C. Flassbeck, K. Wieghardt, *Anorg. Allg. Chem.* **1992**, *608*, 60-68.

[2] A. Company, L. Gómez, M. Güell, X. Ribas, J. M. Luis, L. Que Jr., M. Costas, *J. Am Chem. Soc.* **2007**, *129*, 15766-15767.

[3] A. Company, L. Gómez, X. Fontrodona, X. Ribas, M. Costas, *Chem. Eur. J.* **2008**, *14*, 5727-5731.

[4] I. Prat, D. Font, A. Company, K. Junge, X. Ribas, M. Beller, M. Costas, *Adv. Synth. Catal.* **2013**, *355*, 947-956.